water

MDPI

Article

A Laboratory Scale of the Physical Model for Inclined and Porous Breakwaters on the Coastline of Soc Trang Province (Mekong Delta)

Chuong Thanh Le [1], Duong Van Do [1], Duong Binh Nguyen [1] and Ping Wang [2,*]

[1] Southern Institute of Water Resources Research, Ho Chi Minh City 70000, Vietnam
[2] Institute of Geographic Sciences and Natural Resources Research, Chinese Academy of Sciences, Beijing 100101, China
* Correspondence: wangping@igsnrr.ac.cn

Abstract: In the last few decades, the Mekong Delta coastlines have suffered serious erosion. Strong waves during the Northeast Monsoon are one of the main reasons for this. Many types of breakwaters with different structural components have been designed and built to mitigate coastline erosion. Vertical seawalls have been widely used, but they create reflection waves, which can generate water particle kinematics in front of the structure and increase the toe scour. In this study, an innovative block of inclined and porous breakwaters was studied by conducting laboratory-scale experiments. The experimental results show that inclined and porous breakwaters can considerably reduce wave energy due to transmission, reflection, and diffraction compared to inclined breakwaters. The porosity on the front and back sides of the structures has also been studied. Letting sediment-laden seawaters penetrate inside the sheltered zones, porous breakwaters promote accretion and facilitate the forestation of mangrove belts.

Keywords: Mekong Delta; coastal structure; porous breakwater; Ca Mau Peninsula

Citation: Le, C.T.; Do, D.V.; Nguyen, D.B.; Wang, P. A Laboratory Scale of the Physical Model for Inclined and Porous Breakwaters on the Coastline of Soc Trang Province (Mekong Delta). *Water* **2023**, *15*, 1366. https://doi.org/10.3390/w15071366

Academic Editors: Chin H Wu and Kim Dan Nguyen

Received: 28 February 2023
Revised: 20 March 2023
Accepted: 28 March 2023
Published: 1 April 2023

1. Introduction

Soc Trang Province is on the Ca Mau Peninsula (Mekong Delta) with over 72 km of coastline. Satellite image processing (from Landsat, Sentinel, and Google Earth sources) (Figure 1) shows that in the period 2006–2010, over 295 ha of land and nearly 58 km of coastline were eroded because of the strong waves in the South China Sea (especially during the Northeast Monsoon from November to March).

To address this problem, the Vietnamese Government (through the Ministry of Science and the Ministry of Agriculture) started a research project called "Research on reasonable solutions and technology to prevent erosion and stabilize the coast on the Ca Mau Peninsula" looking for defence systems to prevent coastal erosion. Mangrove forest belts can be considered a nature-based solution to sustainably protect coastal zones from erosion. The local authorities would like to restore these mangrove belts. However, other soft and/or hard measures should be implemented first.

The defence of coastlines against erosion is one of the most troublesome problems. Different defence structures are used around the world (e.g., seawalls, groins, and offshore breakwaters) to prevent shorelines from wave-induced erosion. Each defence structure has advantages and disadvantages, depending on the site-specific conditions. Vertical seawalls have been widely used around the world. However, they can create significant wave reflections. Note that when the wave impinges on the seawall, it forms an ascending jet known as an upward-deflected breaker. Later, the water depth near the seawall runs down during the reflection of the waves and generates a descending vertical jet. This jet produces fluidised sediment at the toe and the resulting scour erosion in the long term (Uh-Zapata et al., 2021) [1]. To overcome this difficulty, inclined seawalls were

introduced. They have efficient energy dissipation compared to vertical seawalls, especially when the slope is gentle. Due to the slope of the seawall, reflective waves are out of phase, allowing some of the incident wave energy to dissipate. The amount of wave energy dissipation depends on the slope provided. The gentler the seawall slope, the more waves break by overtopping, and the more kinematic reduction of water particles (Neelamani and Sandhya, 2003) [2]. Tofany et al. (2014) [3] numerically showed that the scour/deposition patterns at the bottom are formed differently due to different breakwater steepness. As the slopes become gentler, the magnitudes of the scour depth and deposition ridge decrease, and their locations are shifted closer to the breakwater's toe. Based on an extensive database of over 4000 data points, Zanuttigh and van der Meer (2008) [4] analysed wave reflection for various types of coastal structures in design conditions, such as smooth, rock, and armour unit slopes. They developed a new simple formula that relates the reflection coefficient to the breaker parameter. This formula seems to fit all kinds of revetment materials by changing the two coefficients. These coefficients depend only on the correct roughness factor, provided by recent research on overtopping discharges. D'Angremond et al. (1997) [5] critically examined existing data on wave transmission to obtain a homogenous database. These data have been reanalysed, and an expression has been derived relating the transmission coefficient to structural parameters and wave parameters. Koley Santanu et al. (2020) [6] studied regular water wave interactions with Rubble-Mound Offshore Breakwaters (RMOBs). The porosity of the RMOB is uniform, and the breakwaters are placed on a uniform seabed. Compared to a submerged RMOB and an RMOB with its crest level at the SWL (Still-Water Level), an emergent RMOB can effectively reduce wave transmission. This study also suggests that 90% of incident wave energy can be dissipated using RMOBs with 46% porosity. Inspired by the research on Bragg's resonant reflection in wave transmission processes over a sea bottom with ripples, Huan-Wan Liu et al. (2015) [7] and Junliang Gao et al. (2021) [8] have shown that Bragg's resonant reflection can significantly alleviate harbour resonance, thus reducing wave energy. The mechanism of Bragg-type systems with triangular, sinusoidal, and trapezoidal bars has been examined and proposed. The research concentrated on the relationship between peak Bragg resonant reflection and variables like the number of bars (N), bar width (W), and water depth (H). Gao et al. (2020) [9] have studied the capability of focused transient wave groups to trigger the harbour resonance phenomenon and hence mitigate wave energy. They found that factors such as spectral width parameter, incident wave direction, and resonant mode have significant effects on different resonant wave parameters (including maximum runup and resonant intensity of various resonant modes inside a harbour).

Inclined and porous seawalls have a high potential of being a solution to the Vietnamese coastal erosion problem. The major advantage of inclined and porous breakwaters is that they can not only appropriately dissipate wave energy but also minimise wave reflection. They trap wave energy inside the breakwater structure and minimise the load on the structure itself. Porous breakwaters, while letting sediment-laden water penetrate through them, promote sediment accretion inside the sheltered zone and facilitate the forestation of mangrove belts. Another important advantage is that porous breakwaters can be used in many areas with weak soil conditions. This kind of breakwater has been studied very little in the literature.

Tu Le Xuan et al. (2020) [10] proposed Pile–Rock Breakwaters (PRBWs), which comprise a frame of two rows of piles infilled with rock rubble. PRBWs have several advantages that make them particularly applicable to the west coast of Ca Mau and the Mekong Delta. More recently, Tu Le Xuan et al. (2022) [11] introduced a new structure of hollow triangle breakwaters (HTBs) to protect the coastline, stimulate sedimentation, and restore mangrove forests along the Mekong Delta coastline. The hydraulic parameters of the HTB were studied and tested on physical models. These experiments included changing a range of parameters, including the porosity of the surface, wave parameters, and water level, to determine the optimal porosity for wave transmission, reflection, and wave dissipation. The results show that the reflection coefficient is inversely proportional to the breakwater

porosity screen. The transmission coefficient for a non-overtopped breakwater depends on the breakwater porosity screen on both sides of the HTB. Recently, Nguyet-Minh Nguyen et al. (2022) [12] studied three kinds of breakwaters: Pile–Rock Breakwaters (PRBWs), hollow triangle breakwaters (HTBs), and Semicircular Breakwaters (SBWs). The experimental results indicate that the shape and structural design of offshore breakwaters can have a significant influence on the bed morphology in both the seaside and the leesides. In general, the toes of constructions along the seashore are eroded because of reflected waves, and the flow of water is narrowed as it passes through the construction, increasing the speed of the flow and causing erosion. Comparing the breakwater designs, the experimental results show that the HTB has the maximum accretion rate behind the structure, as well as the fastest accretion rate behind the breakwater. The SBW has high wave energy dissipation efficiency, although the toe erosion rate is faster than the other classes of breakwaters. The PRBW shows the fastest toe erosion rate in front of the structure and causes accretion at the leeside of the construction but at a lower rate than the HTB.

Figure 1. Coastal zone satellite image processing of Soc Trang province from 1980 to 2018 (Google Earth).

This paper aims to present a laboratory-scale experiment to assess the capacity of a newly developed design of inclined and Porous Trapezoidal Pyramid Breakwaters, called PTPBWs to reduce wave energies due to transmission, reflection, and diffraction waves. We need to keep in mind that letting sediment-laden waters penetrate inside the sheltered zone to facilitate accretion is also an expected goal of PTPBWs. The impacts of porosity on both the front and the back sides of the wave-reducing capacity are discussed in this study (Figure 2).

Figure 2. Location of expected construction (Google Earth).

2. Breakwater Block Designs

A block of 2 breakwater segments (each 120 m) was planned in the coastal zone of the Lai Hoa commune, Vinh Chau District, Soc Trang, as the structural prototype.

2.1. Water Level and Wave Condition

The design water levels for defining the breakwater crest level are presented in Table 1.

Table 1. Design wave for the structure prototype location.

Simulation Cases	Water Level (m)	Design Deep-Water Monsoon Wave: H_s = 3.03 m, T = 5.82 s	
		H_s (m)	$T_{m\text{-}1,0}$ (s)
Tide level of Probability P = 1%	1.53	0.81	4.83

Deep wave parameters in particular monsoon conditions were determined from a numerical spectral wave model (Le Thanh Chuong and Nguyen Cong Phong, 2019) [13]: the deep-water wave height: $H_s = 3.03$ m; the deep-water wave periods: $T_p = 5.82$ s; and the angle of the incident wave: $\alpha = 70°$ (Figure 3).

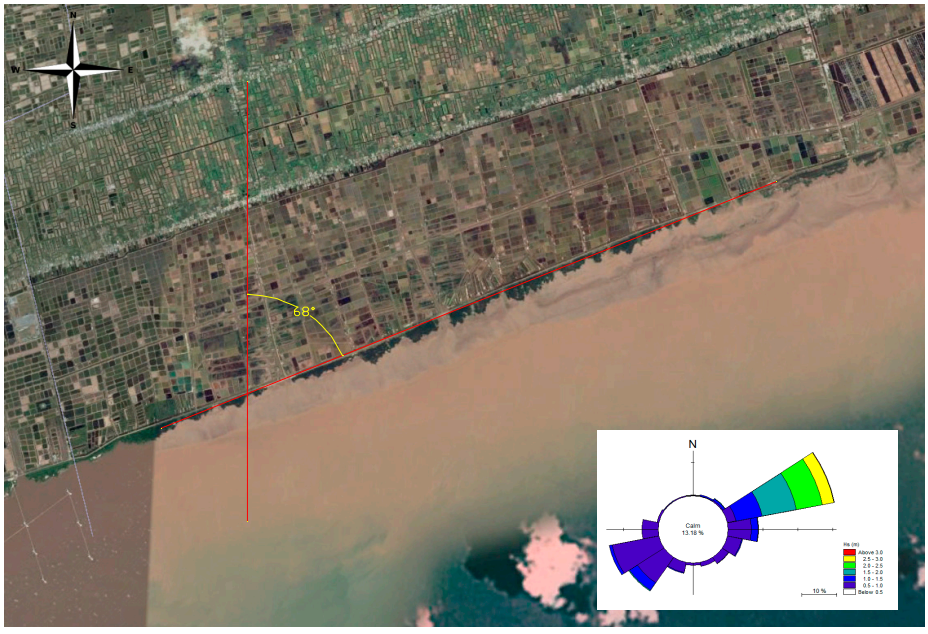

Figure 3. Deep water wave rose 30 km from the shore (MIKE 21 SW).

The final design parameters for the prototype are the wave parameters in the water-level condition of probability P = 1%: the water depth in the prototype construction is 2.03 m; the wave height is H_{m0} = 0.81 m; the wave period is $T_{m-1,0}$ = 4.83 s; the wave length is L_m = 25.0 m; and the wave steepness is $S_{op} = H_{m0}/L_m$ = 0.032.

2.2. Breakwater Parameters

According to the Vietnamese Structure Design Standard TCVN-9901:2014—Hydraulic structures [14], a few crest values were selected as follows:

2.2.1. Submerged Breakwater

The crest level for the submerged breakwater is calculated as

$$Z_s = Z_{tp} - 1/2H_s + S = +1.62 \text{ m};$$

where Z_{tp} is the sea water level, $Z_{tp} = Z_{1\%}$ = +1.53, H_s = 0.81 m is the wave height at the expected construction area, and the planned subsidence height S = 0.5 m.

2.2.2. Emerged Breakwater

The crest level for the emerged breakwater is calculated as

$$Z_e = Z_{tp} + 1/2H_s + S = +2.44 \text{ m}$$

Finally, the final crest level of the prototype is +2.0 m, and the structure height is 2.50 m. The block weight of a PTPBW block is 10.14 tons. Details on the dimensions of the PTPBW block are given in Figure 4.

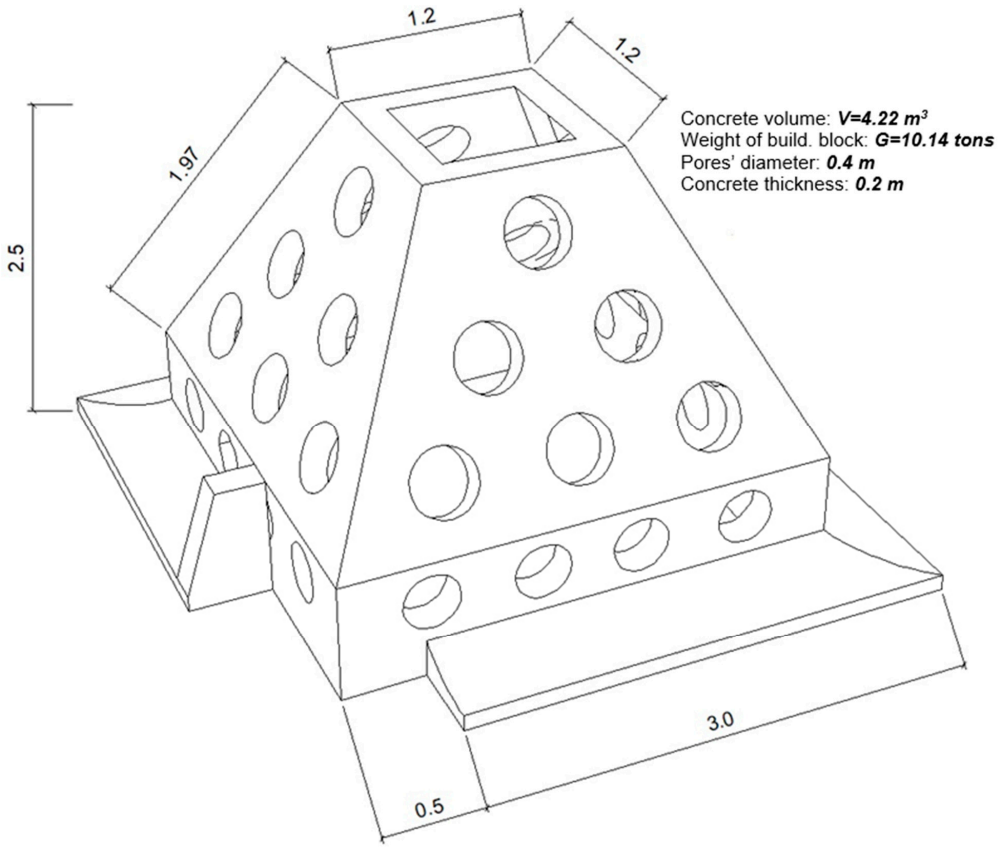

Figure 4. Dimensions of a PTPBW block.

3. Physical Models

3.1. Modelling Scales

The physical model was performed in the wave flume of the Coastal Hydrodynamics Laboratory of the Southern Institute of Water Resources Research (CHL/SIWRR, Vietnam).

The model scales were determined depending on the hydrodynamic boundary conditions (wave, water depth) and the wave flume capacity (maximum generated wave height and the dimension of the flume). In addition, the model was constructed on the basis of the Froude similarity to ensure the same hydrodynamic conditions as the prototype model. The crest freeboard *Rc* of the prototype ranges within ($\pm 1/2 H_{s,\max}$) (Figure 5).

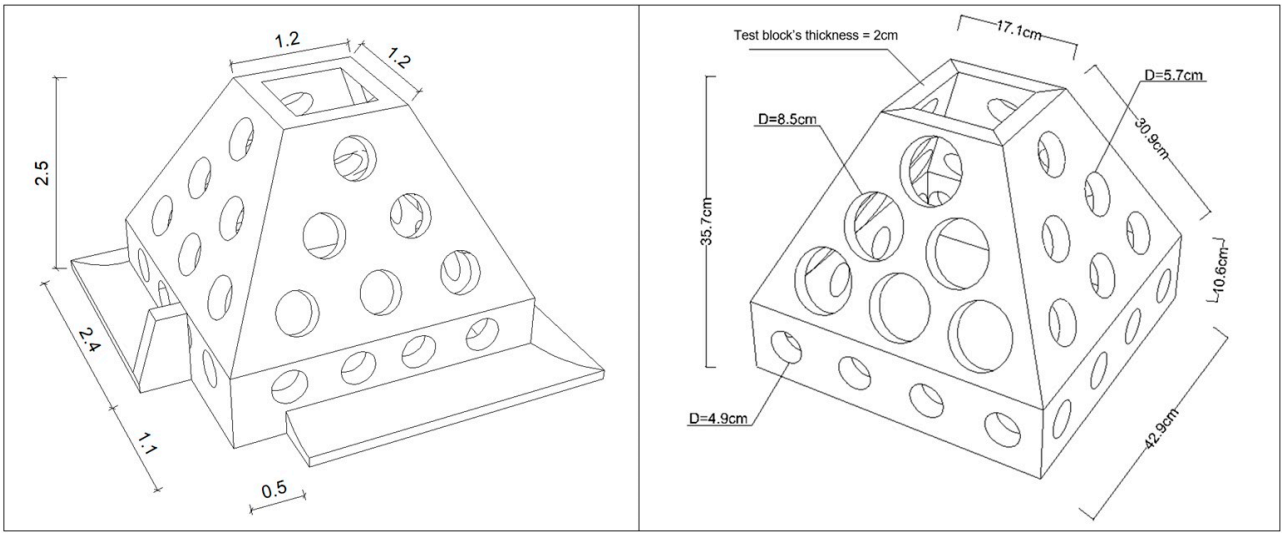

Figure 5. Size of the prototype PTPBW block and physical modelling.

The physical model must ensure incident waves with heights varying from 0.5 m to 2 m and periods varying from 5 s to 7 s. The water depths of the physical model must reflect the range of the tidal water at the prototype location (from 1.5 m to 3.5 m). In addition, it must be ensured that the model scale value's impact on the results is minimal. On the basis of the wave flume capacity, the length scale of the model was chosen as 7. Therefore, the time scale that was calculated from the Froude similarity is 2.65 (Table 2). The form of the physical-model block is identical to that of the design prototype, which is an inclined and porous breakwater with a length ratio of 1/7. The wave-generating paddles were programmed and controlled with HR Wallingford software (HR Wallingford, 2008) [15] using the Jonswap spectrum formula (Figure 6).

Table 2. Model scale.

Model Scale	Value
Length scale N_L	7
Time scale N_t	2.65

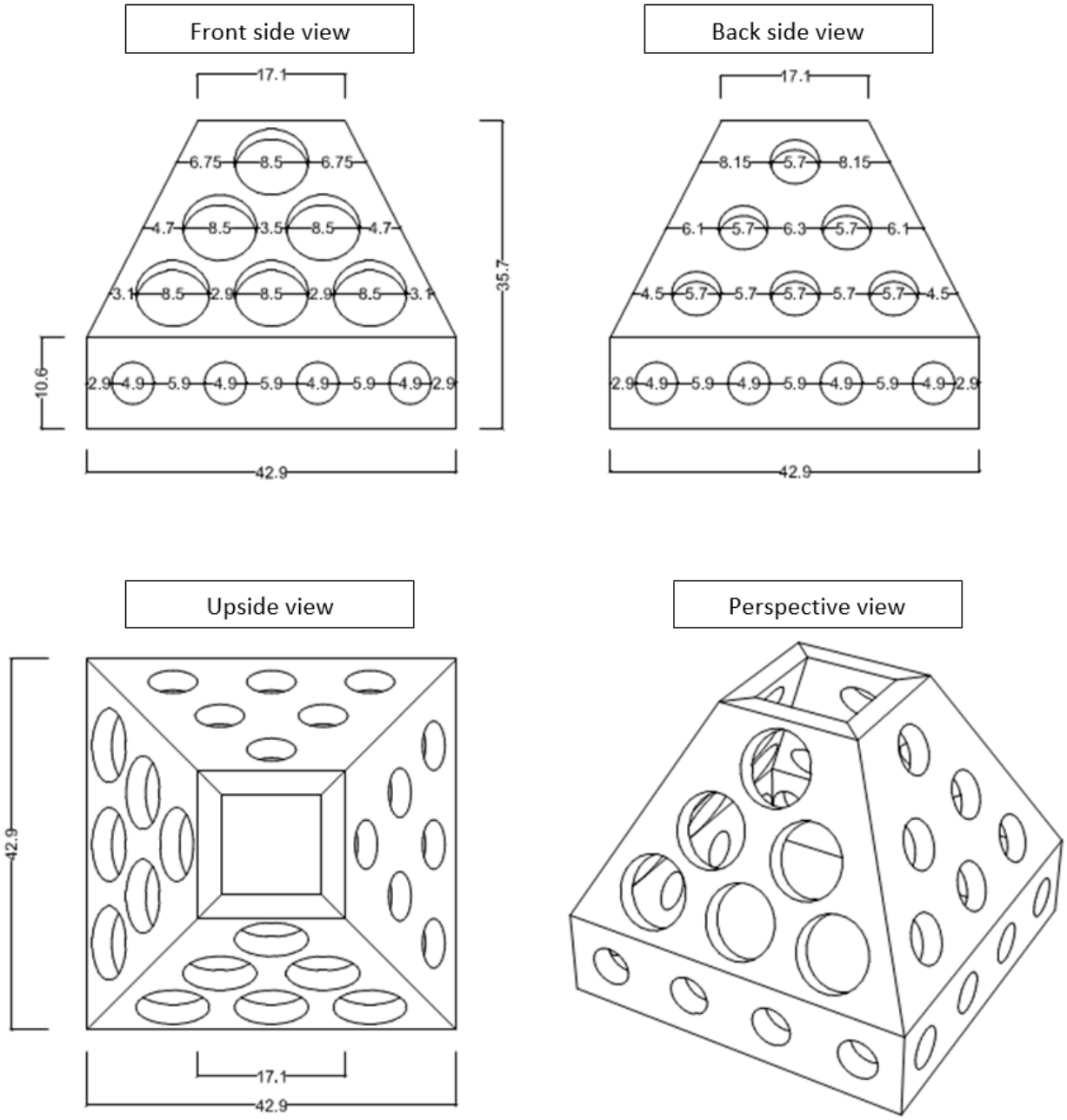

Figure 6. Size of the prototype PTPBW block (unit: cm).

3.2. Model Construction and Scenarios

Eight wave gauge sensors were set up in front of and behind the PTPBW block. Five sensors were in front of the structure (WG1, 2, 3, 4, 5) and were used to measure incident waves. Four of them were used to decompose reflected waves from the incident wave. Behind the structure, sensors (WG6, 7, 8) were used to measure the transmitted waves after passing the inclined and porous structure. The positions of the sensors are depicted in Figure 7. The wave frequency spectra were extracted in diapason from 0.01 Hz to 2.5 Hz with a measuring scale of 0.01 s/value.

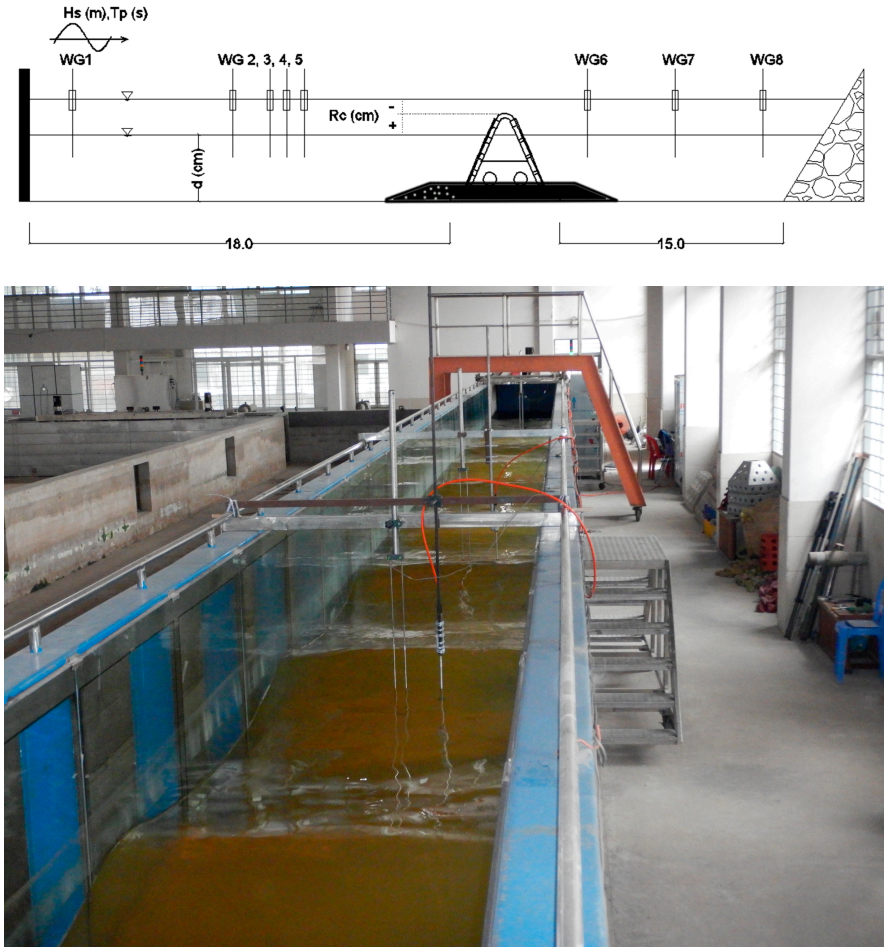

Figure 7. Wave flume in the Coastal Hydrodynamics Laboratory of SIWRR.

The block of the physical model was constructed with wood materials for simplicity in setting up and changing between scenarios. Wave energy dissipation caused by the structure forces the wave to break; thus, the use of wood materials has no influence on the physical model's results (Figure 8).

Figure 8. Setting up the model block in the wave flume.

The stone revetment has a slope of 0.5 and a streamwise length of 40 cm from the breakwater toe (Figure 9).

Figure 9. Design of stone revetment for scour protection.

Comparisons between inclined breakwaters with and without pores were performed. Model construction was performed in two steps:

- Defining an optimal diameter of the pores in the breakwater surfaces; the pores could be on either the front or the back side or on both sides;
- Defining the wave energy dissipation ability of the block with chosen pores (presented in Table 3 below).

Table 3. Diameters of the physical test cases.

No	Experimental Model Pore Diameter	Prototype Pore Diameter
1	D = 4.1 cm	D = 30 cm
2	D = 5.7 cm	D = 40 cm
3	D = 7.3 cm	D = 50 cm
4	D = 8.9 cm	D = 60 cm

The pore alternating process was performed using micanite rings, with a design principle in which the inner circle of the outer ring equals the outer circle of the inner ring, thus ensuring tightness during the test. For each pore on the front side, 3 rings were sequentially used to present 4 diameters for 4 test cases, as shown in Figure 10. The outermost ring has an outer diameter of 8.9 cm, and the inner ring has an outer diameter of 7.3 cm. The second ring has an outer diameter of 7.3 cm and an inner diameter of 5.7 cm. The innermost ring has an outer diameter of 5.7 cm and an inner diameter of 4.1 cm.

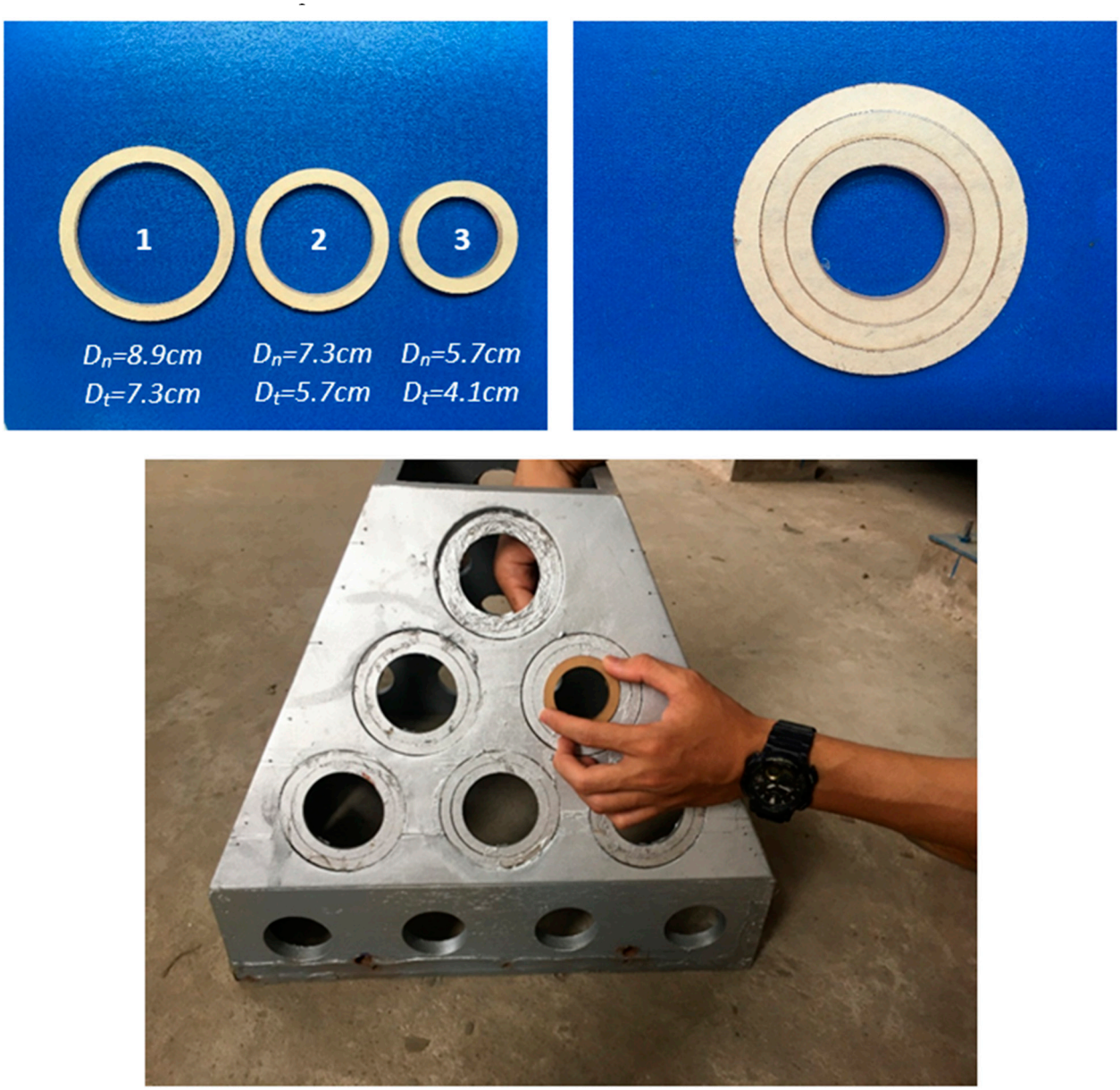

Figure 10. Sizes of the rings composing the pore in the model block (D_o—outer diameter; D_i—inner diameter). 1—Outer and inner rings for pore emulation in the breakwater. 2—Rings are combined together to achive the necessary pore diameter. 3—Putting the combined rings to the breakwater phisical model.

- On the back side, the diameter of the largest pore is 5.7 cm, whereas the diameter of the smallest pore is 4.1 cm.
- On the front side, the diameter of the largest pore is 8.9 cm. It is 5.7 cm for the smallest pore.

The percentages of the pores on the front side and the back side in the different scenarios are presented in Table 4. Note that TH3 is the case without pores on the front side. Table 5 defines the test cases for finding the optimal pore diameter of a PTPWB. According to a matrix combination of the element numbers in the 3 columns of this table (6,2,4), the number of test cases is 48. Similarly, according to the elements (2,4,5) in the 3 columns in Table 6, the number of test cases for assessing wave dissipation capacities is 40.

Table 4. Pore percentages in the experimental block surface in test cases.

Test Cases	Front-Side and Back-Side Pore Diameter (cm)	Front-Side Pore Percentage (P_1)	Back-Side Pore Percentage (P_2)
TH2	Di = 8.9 cm; D_s = 5.7 cm	34.2%	17.6%
TH3 (without pore on front side)	Di = 0.0 cm; D_s = 5.7 cm	0.0%	17.6%
TH4	Di = 5.7 cm; D_s = 5.7 cm	17.6%	17.6%
TH5	Di = 7.3 cm; D_s = 5.7 cm	25.0%	17.6%
TH6	Di = 5.7 cm; D_s = 4.1 cm	17.6%	12.0%
TH7	Di = 7.3 cm; D_s = 4.1 cm	25.0%	12.0%

Table 5. Scenarios for finding the optimal pore diameter.

Test Cases	Front-Side and Back-Side Pore Diameter (cm)	Water Depth d (cm) Crest Freeboard R_c (cm)	Wave Parameters
TH2	Di = 8.9 cm; D_s = 5.7 cm	d = 47 cm (Rc = 0 cm) d = 33 cm (R_c = +14 cm)	H_s = 0.1 m; T_p = 1.5 s H_s = 0.1 m; T_p = 2.5 s H_s = 0.14 m; T_p = 1.5 s H_s = 0.14 m; T_p = 2.5 s
TH3	Di = 0.0 cm; D_s = 5.7 cm		
TH4	Di = 5.7 cm; D_s = 5.7 cm		
TH5	Di = 7.3 cm; D_s = 5.7 cm		
TH6	Di = 5.7 cm; D_s = 4.1 cm		
TH7	Di = 7.3 cm; D_s = 4.1 cm		

Table 6. Test cases for assessing wave dissipation capacities.

Test Cases	Water Depth d (cm) Crest Freeboard R_c (cm)	Wave Parameters
No structure	d = 47 cm (Rc = 0 cm) d = 40 cm (Rc = +7 cm) d = 33 cm (R_c = +14 cm) d = 26 cm (R_c = +21 cm)	H_s = 0.07 m; T_p = 1.2 s H_s = 0.10 m; T_p = 1.5 s H_s = 0.12 m; T_p = 1.6 s H_s = 0.14 m; T_p = 1.7 s H_s = 0.17 m; T_p = 1.8 s
With structure		

4. Results and Discussion

4.1. Wave Parameter Estimations

The wave parameters (heights, periods) in front of and behind the block were analysed according to wave spectral density using HR Wallingford software (HR Wallingford, 2008) [15]. The program decomposes reflected waves on the basis of the Mansard and Funke methods (Mansard and Funke, 1980) [16] to define incident waves ($H_{m0,i}$) and reflecting waves ($H_{m0,r}$) in front of the structure using four sensors (WG2, 3, 4, 5).

The parameters measured during the whole physical model are presented below (see the table of notations given at the end of this document for the definitions of different parameters):

❖ Wave height at zero moment H_{m0}

The wave height at zero moment H_{m0} can be defined using the zero moment of the wave variance density spectra (Nguyen Viet Tien et al., 2013) [17]:

$$H_{m0} = 4.004\sqrt{m_0} = 4.004\sqrt{\int_{f\min}^{f\max} S(f)df} \quad (1)$$

- $S(f)$ is the variance density of the spectrum corresponding to frequency f;

$$S(f) = \frac{\beta g^2}{16\pi^4} f^{-5} \exp\left[-\frac{5}{4}\left(\frac{f}{f_m}\right)^{-4}\right]\gamma^b$$

where $b = \exp\left[-\frac{1}{2\sigma^2}\left(\frac{f}{f_m} - 1\right)^2\right]$

$\sigma = \begin{cases} \sigma_1 & , f \le f_m \\ \sigma_2 & , f > f_m \end{cases}$

σ_1, σ_2—Spectral width parameters.

❖ Wave peak periods T_p and $T_{m-1,0}$

$$T_{m-1,0} = \frac{m_{-1}}{m_0} = \frac{\int_{f\min}^{f\max} f^{-1} S(f) df}{\int_{f\min}^{\max} S(f) df} \quad (2)$$

❖ Wave transmission coefficient of the breakwater

The wave-reducing effects of the breakwater were evaluated using the ratio between the wave heights behind and in front of the structure.

The wave-reducing effect is calculated as:

$$\varepsilon = 1 - K_t$$

$$K_t = \frac{H_{m0,t}}{H_{m0,i}} \quad (3)$$

where K_t is the wave transmission coefficient;

Crest freeboard (R_c) is the distance from the breakwater crest to the water surface. with $R_c > 0$ for emerged breakwaters and $R_c < 0$ for submerged breakwaters (Figure 7, Top).

❖ Wave reflection coefficient

$$K_r = \frac{H_{m0,r}}{H_{m0,i}} \quad (4)$$

❖ Wave dissipation coefficient

When interacting with the structure, the energy of the incident wave (E_i) is transformed into the reflection wave energy (E_r), dissipated wave energy (E_D), and transmission wave energy (E_t):

$$E_i = E_r + E_D + E_t \quad (5)$$

The result of the energy transformation can also be presented using the wave reflection coefficient (K_r), wave dissipation coefficient (K_D), and wave transmission coefficient (K_t). Two equations below show the dependencies between these variables (Nguyen Viet Tien et al., 2013):

$$1 = K_r^2 + K_D^2 + K_t^2 \cdots \Leftrightarrow \cdots K_D = \sqrt{1 - \left(K_r^2 + K_t^2\right)} \quad (6)$$

4.2. Dependency of Wave Dissipation Capacity on Pore Diameters of Breakwater

The selection of a pore diameter depends on the stress-bearing specification, wave transmission coefficient (K_t), wave reflection coefficient (K_r), and wave dissipation coefficient

(K_D) of the block. The selected pore diameter should give the highest value of K_D. The pore diameters on both the front and back sides have been taken into consideration.

The wave reflection coefficient K_r in relation to R_c is given in Figure 11a. In the case without pores, the K_r of scenario TH3 is (0.25–0.35), which is much higher than that of the other scenarios. This result is as expected because the inclined breakwaters without pores produce a higher reflected wave energy than the other scenarios.

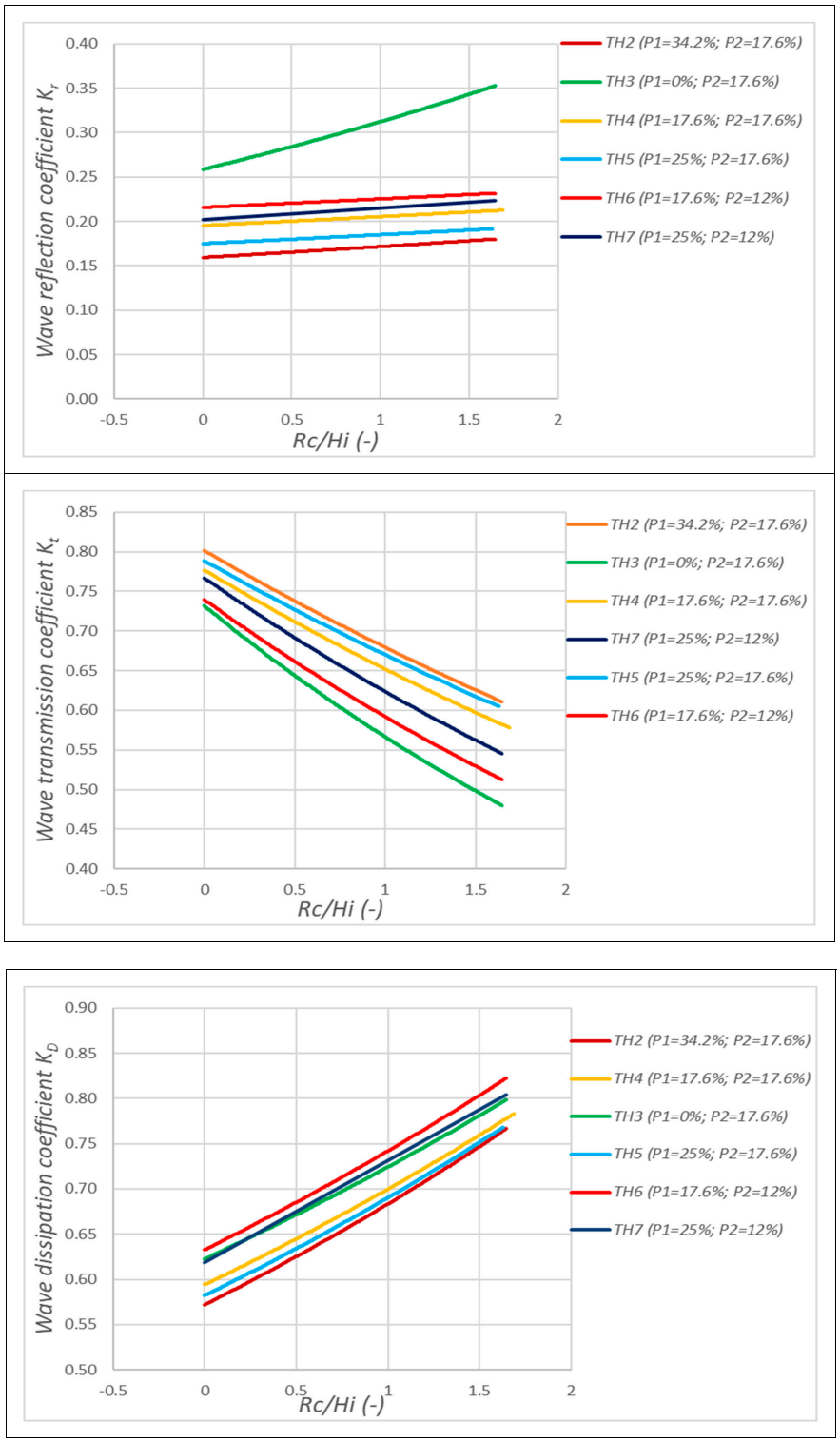

Figure 11. Influence of the crest freeboard of the PTPBW on the coefficients K_r, K_t, and K_D.

In the cases with pores, the steepness of the graphs is weak; thus, the change in the wave reflection coefficient K_r is tiny with the changing crest freeboard (R_c). K_r is always smaller than 0.25; thus, the design of the breakwater significantly reduces erosion due to reflection waves (one of the main reasons for breakwater damage). Note that the larger the diameter on the front side, the smaller the value of K_r. TH2, with the largest pore diameter, has the smallest K_r value. The pore diameter on the back side also influences the wave reflection coefficient. TH4 and TH6 have the same pore diameter on the front side, but TH6 has a value of K_r that is higher than that of TH4 because the pore diameter on the back side in TH6 is smaller.

The wave transmission coefficient K_t is depicted in Figure 11b. With the crest freeboard R_c changing within a range of (0–21 cm), the wave transmission coefficients vary within (0.48–0.80), and the wave energy behind the structure is five times smaller. When the porosity of the back side is 17.6% and the porosity of the front side is 34.2% (TH2), the wave-reducing capacity is lowest. The wave-reducing capacity is best when one side is impermeable (no pores). To minimise reflected waves, all sides of the structure should be permeable (i.e., porous). The best wave-reducing capacity was reached when the porosity of the front side was 17.6% and that of the back side was 12% (TH6).

When we have K_r and K_t, K_D can be determined with (7), as summarised in Figure 11c. According to Figure 11c, when the porosity on the front side is 34.2% and that on the back side is 17.6% (TH2), the wave dissipation capacity is lowest. The structure has the best wave dissipation capacity when the front-side porosity is 17.6% and the back-side porosity is 12%. Therefore, TH6 is selected as having the optimal porosity.

4.3. Wave-Reducing Effects

The above-selected pore diameter (TH6, front-side porosity is 17.6%, D = 5.7 cm, and the back-side porosity is 12%, D = 4.1 cm) was used to check the wave dissipation effects under different wave and water depth conditions.

With the selected pore parameters, the wave transmission coefficient oscillates in a range of (0.3 ÷ 0.8) for different cases of waves and water depths, corresponding to the wave dissipation effects varying within (20% ÷ 70%). The wave transmission coefficient is reduced linearly with the crest freeboard, R_c (Figure 12). The best wave dissipation coefficient achieved 70% when the crest freeboard was $R_c = +21$ cm, equivalent to R_c/H_{m0} varying within (2.60~3.56).

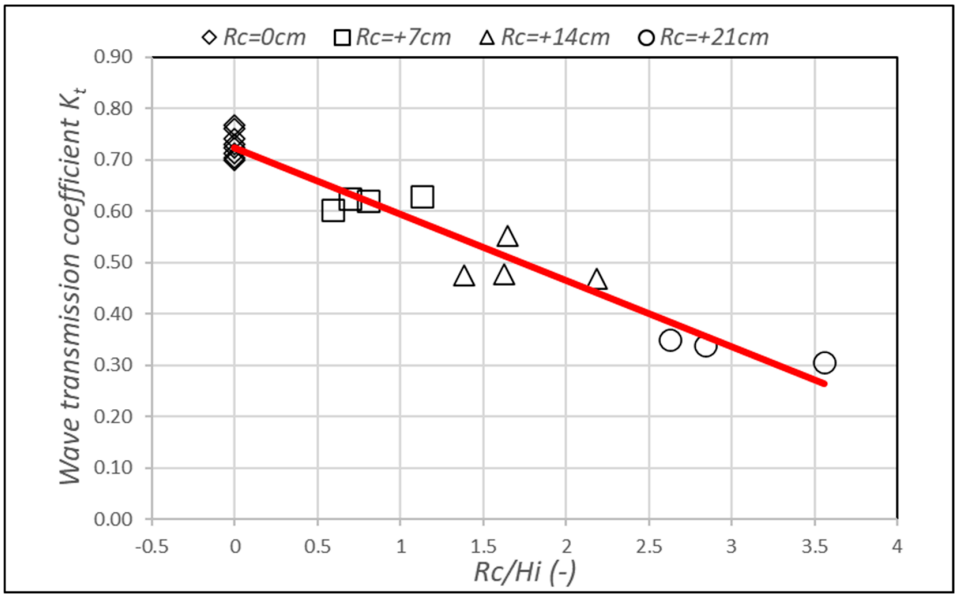

Figure 12. Influence of the crest freeboard on the wave transmission coefficient K_t.

Figure 13 provides a comparison of wave transmission coefficients versus relative crest freeboards of different types of breakwaters. A comparison of the K_t values between the HTB, PRWB, and rubble-mound breakwaters reveals that the transmission efficiency is low when the breakwaters are working in the emerging state. However, when breakwaters are submerged, the transmission coefficient of the rubble mound has the lowest value, with $K_t < 0.2$. Rubble-mound breakwaters almost completely prevent incoming waves. Porous breakwaters, like HTBs and PRBWs, still enable waves to pass through the layer to a certain degree, and the transmission coefficients are almost unchanged, $K_t = 0.3$–0.4. The PTPBW results presented in this figure correspond to the selected pore diameter (TH6, front-side porosity is 17.6%, $D = 5.7$ cm, and the back-side porosity is 12%, $D = 4.1$ cm). We note that although we favour the penetration of sediment-laden waters, the proposed PTPBW structure gives values of wave transmission coefficients that are comparable with the other structures. When $R_c/H_{mo,i} > 2$, the wave transmission coefficients given by the PTPBWs are nearly identical to those of the HTBs and PRBWs. This ensures that the main purpose of the PTPBWs is to facilitate sediment transport along the structure and stimulate sedimentation behind it.

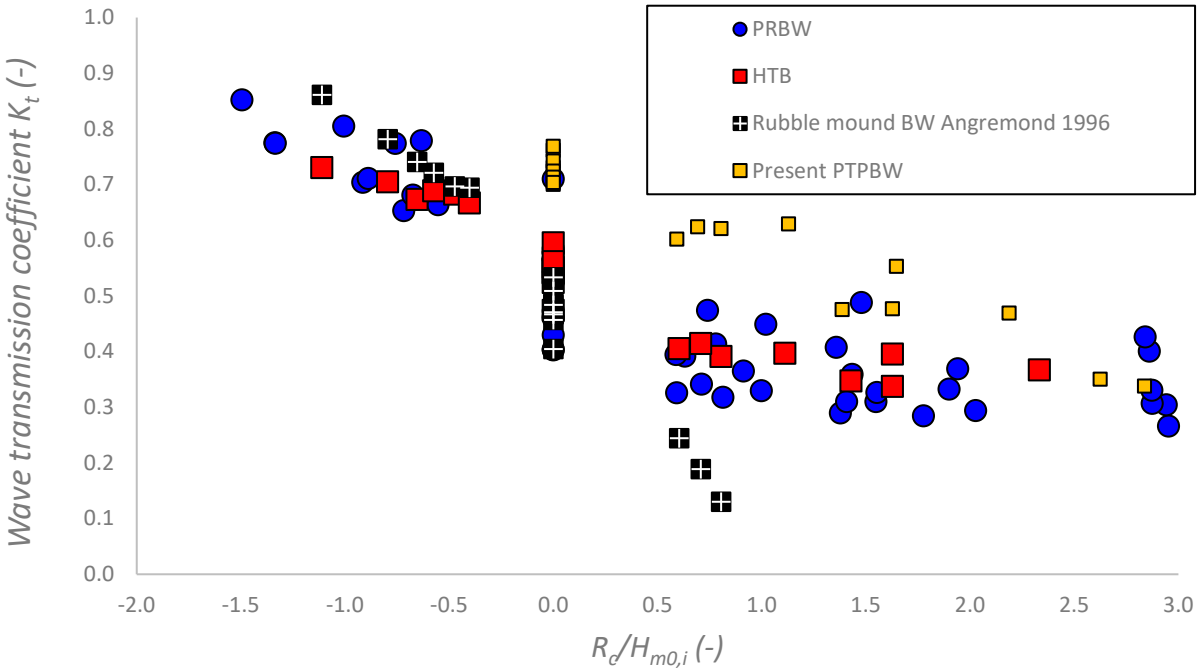

Figure 13. Wave transmission coefficients versus relative crest freeboards of different types of breakwaters: PRBW (Le Xuan Tu et al., 2020) [10], HTB (Le Xuan Tu et al., 2022) [11], rubble-mound BW (D'Angremeond, 1997) [5], and present PTPBW.

With the designed PTPBW block, the reflection wave energy is relatively small, as shown by the wave variance spectrum depicted in Figure 14 (the blue line shows the density spectrum of the incident wave, and the black lines show the density spectrum of the reflected wave). The density of the reflected wave is still small even though the water depth increases nearly two times (from 26 cm to 47 cm).

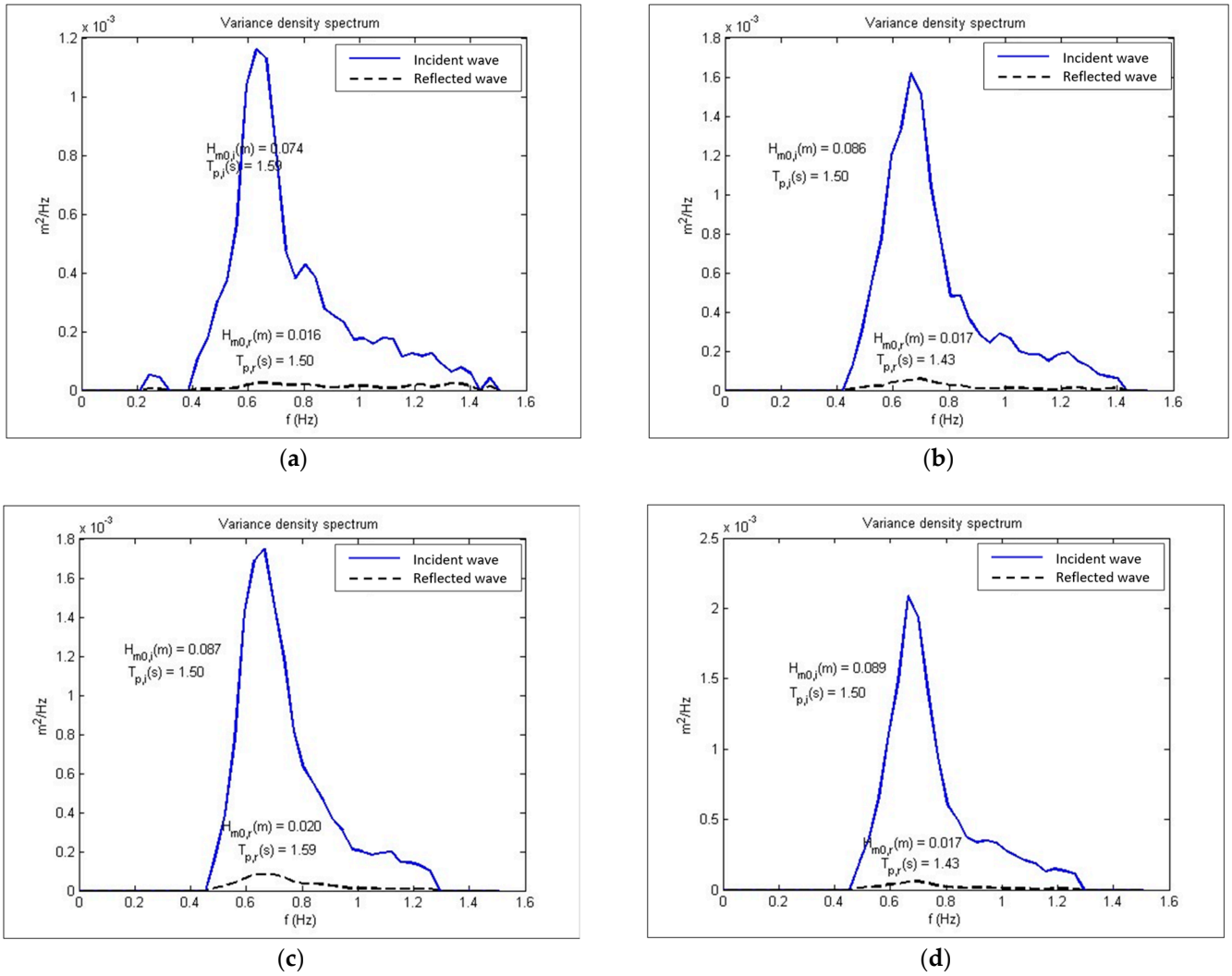

Figure 14. Variance spectrum of the reflected wave in different water depths. (**a**) TH6-d26H10T15, Depth d = 26 cm, Variance density spectrum; (**b**) TH6-d33H10T15, Depth d = 33 cm, Variance density spectrum; (**c**) TH6-d40H10T15, Depth d = 40 cm, Variance density spectrum; (**d**) TH6-d47H10T15, Depth d = 47 cm, Variance density spectrum.

The reflection coefficients in front of the structure differ slightly between (0.2 ÷ 0.25), as depicted in Figure 15. With a low water level (wave overtopping does not occur when R_c varies from +14 cm to +21 cm, equivalent to R_c/H_{m0} varying from (1.39~1.63) to (2.60~3.56), respectively) and a high water level (without wave overtopping, R_c varies within +7–0 cm, i.e., R_c/H_{m0} varies from (0.60~1.12) to 0), the reflection coefficients are nearly identical. This means that the designed breakwater dissipates much reflection wave energy.

The relationship between K_r and R_c/H_{m0} is shown in Figure 16. When $R_c/H_{m0} = -1$, i.e., in the emerging state, the wave reflection coefficients converge for all breakwaters with K_r = 0.1–0.2. When the breakwaters work in an emerging state ($R_c > 0$), the proposed PTPWB produced the smallest reflection wave coefficient of K_r = 0.20–0.25. Next is the rubble mound with K_r = 0.26–0.28; the HTB with K_r = 0.35–0.47; and the PRBW with K_r = 0.45–0.56; and the smooth breakwater yielded the largest reflected wave coefficient of K_r = 0.54–0.72.

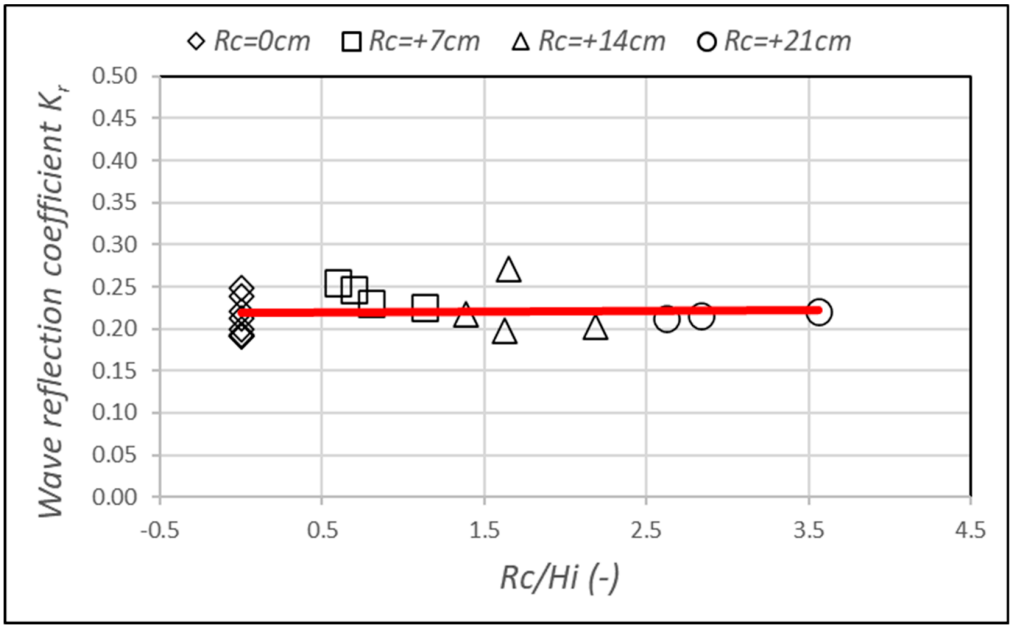

Figure 15. Influence of the crest freeboard on the wave reflection coefficient K_r.

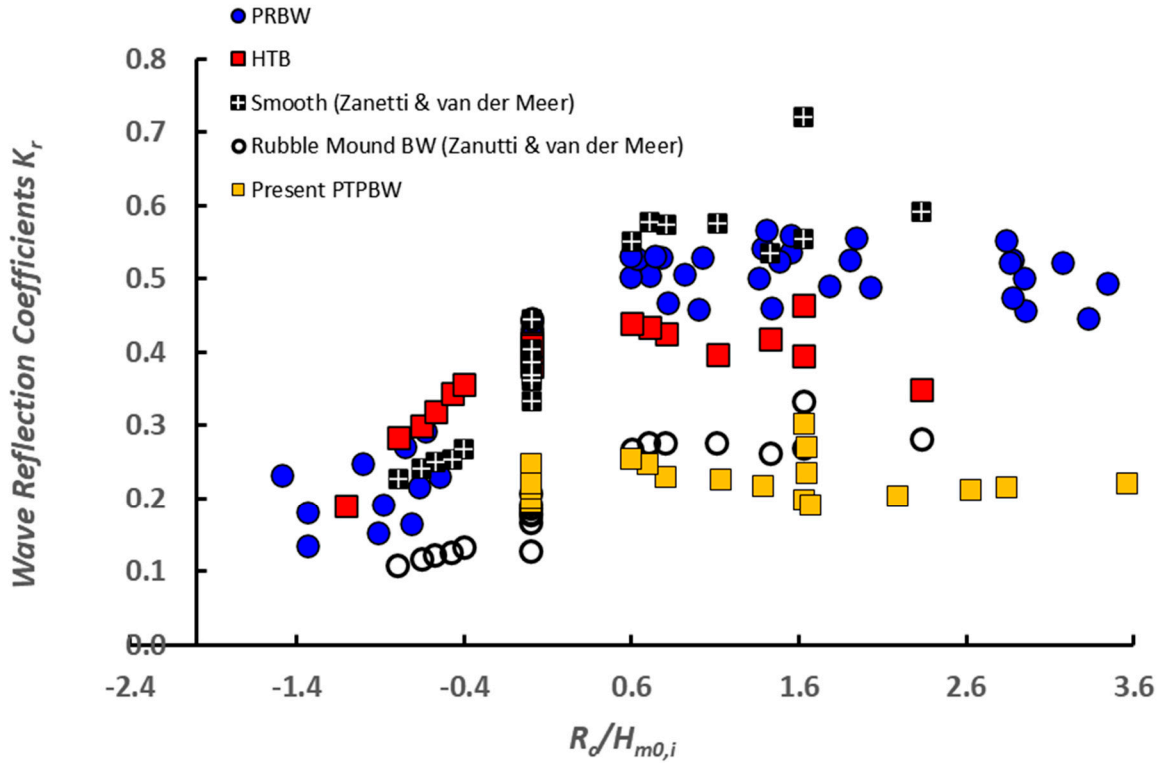

Figure 16. Wave reflection coefficients versus relative crest freeboards of different breakwaters: PRBW (Le Xuan Tu et al., 2020) [10], HTB (Le Xuan Tu et al., 2022) [11], smooth breakwater (Zanutti and van der Meer, 2008) [4], and rubble-mound BW (Zanutti and van der Meer, 2008) [4].

5. Conclusions

The Porous Trapezoidal Pyramid Breakwater (PTPBW) can considerably reduce wave energy in comparison with inclined breakwaters without pores. Minimizing wave reflection, it is the most effective in ensuring sediment transport along the structure and stimulating

sedimentation behind it, compared to PRBWs, HTBs, smooth breakwaters, and rubble mounds.

The 2D physical model used (in a wave flume) can help us define the optimal pore diameters of inclined and porous breakwaters using the wave transmission coefficient, wave reflection coefficient, and wave dissipation coefficients. The optimal pore sizes (5.7 cm and 4.1 cm) obtained from the physical models were then used to evaluate the wave dissipation capacity. The test shows that when the water level is 1 m lower than the crest (R_c = 14 cm in the model), the structure reduces the wave by 50%, and the wave power is reduced tenfold after passing through the breakwater. The reflected wave in front of the structure has a wave height of 1/5 of the incident wave height.

The Mekong coastal zone's geologic foundation is weak, so porous breakwaters have substantial advantages in terms of risk of subsidence in comparison with traditional breakwaters. In Vietnam and around the world, porous breakwaters are relatively novel coastal defence structures. Porous breakwaters are very diverse. Their effectiveness and applicability need to be studied for each region with different wave and soil characteristics. A breakwater system has been designed and built in 2022 on the basis of these experimental results (see Figure 17). Our research results can serve as reference data and experience for forthcoming engineering coastal-protection projects in the Mekong Delta (Vietnam).

Figure 17. Wave breakwaters with PTPBW structure, which was designed on the basis of the present research results.

Author Contributions: Methodology, D.V.D. and D.B.N.; Software, D.B.N.; Validation, D.V.D.; Investigation, C.T.L. and D.B.N.; Writing—original draft, C.T.L., D.V.D. and D.B.N.; Writing—review & editing, P.W.; Funding acquisition, C.T.L. and D.V.D. All authors have read and agreed to the published version of the manuscript.

Funding: This study received grants from the Vietnamese Ministry of Science and Technology (MOST, 08/2017/HD-DTDL.CN-CNN) and the Ministry of Agriculture and Rural Development (MARD).

Institutional Review Board Statement: Not applicable.

Informed Consent Statement: Not applicable.

Data Availability Statement: Not applicable.

Conflicts of Interest: The authors declare no conflict of interest.

Glossary

α—Angle of the incident wave;
β—Spectral energy parameter;
γ—Peak enhancement factor;
D—Pore diameter;
D_o—Outer diameter (of the rings composing the pore in the model block);
D_i—Inner diameter (of the rings composing the pore in the model block);
D_s—Back-side pore diameter;
f_m— Value of pick frequency;
H_s—Deep-water wave height;
H_{m0}—Wave height at zero moment;
$H_{m0,i}$—Incident wave height at zero moment in front of the structure at a distance of 1.5 m from the breakwater;
$H_{m0,r}$—Reflected wave height in front of the structure at a distance of 1.5 m from the breakwater.
K_t—Wave transmission coefficient;
K_D—Wave dissipation coefficient;
K_r—Wave reflection coefficient at the front of the breakwater;
L_m—Wave length;
m_0—Zero moment of the spectrum;
m_{-1}—Zero moment of the spectrum;
N_L—Length scale;
N_t—Time scale;
R_c—Crest freeboard;
S—Planned subsidence height;
$S_{op} = H_{m0}/L_m$—Wave steepness;
T_p—Deep-water wave period;
$T_{m\text{-}1,0}$—Wave period;
Z_{tp}—Sea water level;
$Z_{1\%}$—Sea water level at the probability 1%;
Z_s—Crest level of the submerged breakwater;
Z_e—Crest level for the emerged breakwater.

References

1. Zapata, M.U.; Van Bang, D.P.; Nguyen, K.D. Unstructured Finite-Volume Model of Sediment Scouring Due to Wave Impact on Vertical Seawalls. *J. Mar. Sci. Eng.* **2021**, *9*, 1440. [CrossRef]
2. Neelamani, S.; Sandhya, N. Wave reflection characteristics of plane, dentated and serrated seawalls. *Ocean. Eng.* **2003**, *30*, 1507–1533. [CrossRef]
3. Tofany, N.; Ahmad, M.; Kartono, A.; Mamat, M.; Mohd-Lokman, H. Numerical modeling of the hydrodynamics of standing wave and scouring in front of impermeable breakwaters with different steepnesses. *Ocean Eng.* **2014**, *88*, 255–270. [CrossRef]
4. Zanuttigh, B.; van der Meer, J.W. Wave reflection from coastal structures in design conditions. *Coast. Eng.* **2008**, *55*, 771–779. [CrossRef]
5. d'Angremond, K.; Van Der Meer, J.W.; De Jong, R.J. Wave Transmission at Low-Crested Structures. In Proceedings of the 25th International Conference on Coastal Engineering, Orlando, FL, USA, 2–6 September 1996; ASCE: Reston, VA, USA, 1997; pp. 2418–2427.
6. Santanu, K.; Panduranga, K.; Almashan, N.; Neelamani, S.; Al-Ragum, A. Numerical and experimental modelling of water wave interaction with rubble mound offshore porous breakwaters. *Ocean. Eng.* **2020**, *218*, 108218.
7. Liu, H.-W.; Luo, H.; Zeng, H.-D. Optimal Collocation of Three Kinds of Bragg Breakwaters for Bragg Resonant Reflection by Long Waves. *J. Waterw. Port Coast. Ocean. Eng.* **2015**, *141*, 04014039. [CrossRef]
8. Gao, J.; Ma, X.; Dong, G.; Chen, H.; Liu, Q.; Zang, J. Investigation on the effects of Bragg reflection on harbor oscillations. *Coast. Eng.* **2021**, *170*, 103977. [CrossRef]
9. Gao, J.; Ma, X.; Zang, J.; Dong, G.; Ma, X.; Zhu, Y.; Zhou, L. Numerical investigation of harbor oscillations induced by focused transient wave groups. *Coast. Eng.* **2020**, *158*, 103670. [CrossRef]
10. Le Xuan, T.; Ba, H.T.; Le Manh, H.; Van, D.D.; Nguyen, N.M.; Wright, D.P.; Bui, V.H.; Mai, S.T.; Anh, D.T. Hydraulic performance and wave transmission through pile-rock breakwaters. *Ocean Eng.* **2020**, *218*, 108229. [CrossRef]
11. Le Xuan, T.; Le Manh, H.; Ba, H.T.; Van, D.D.; Vu, H.T.D.; Wright, D.; Bui, V.H.; Anh, D.T. Wave energy dissipation through a hollow triangle breakwater on the coastal Mekong Delta. *Ocean Eng.* **2022**, *245*, 110419. [CrossRef]
12. Nguyen, N.-M.; Van, D.D.; Le, D.T.; Nguyen, Q.; Pham, N.T.; Tanim, A.H.; Gagnon, A.S.; Wright, D.P.; Thanh, P.N.; Anh, D.T. Experimental modeling of bed morphological changes and toe erosion of emerged breakwaters due to wave-structure interactions in a deltaic coast. *Mar. Geol.* **2022**, *454*, 106932. [CrossRef]
13. Chuong, L.T.; Phong, N.C. *Computation of Wave and Water Level Combinations for Physical Model Test*; Southern Institute of Water Resources Research: Ho-Chi-Minh City, Vietnam, 2019.
14. *TCVN-9901:2014*; Hydraulic Structures. Sea Structure Design Standard. Available online: http://tlu.edu.vn/Portals/0/CRA/TCVN%209901.rar (accessed on 16 February 2022).

15. HR Wallingford. *Wave Probe Monitor—User Manual*; HR Wallingford: Wallingford, UK, 2008.
16. Mansard EP, D.; Funke, E.R. The Measurement of Incident and Reflected Spectra Using a Least squares Method. In Proceedings of the 17th International Conference on Coastal Engineering, Sydney, Australia, 23–28 March 1980.
17. Tien, N.V.; Tuan, T.Q.; Truyen, L.K. Research of submerged breakwater and upstream zone effects on wave reducing effects using physical model with wave flume. *J. Water Ressour. Environ. Technol.* **2013**, *4100011*, 69–79. (In Vietnamese)